

1
2
3 **Dosimetry and prescription in liver radioembolization with ^{90}Y microspheres: 3D calculation of**
4 **tumor-to-liver ratio from global $^{99\text{m}}\text{Tc}$ -MAA SPECT information**
5
6
7

8 Fernando Mañeru¹, Dolores Abós^{2, 3}, Laura Bragado¹, Naiara Fuentemilla¹, Fernando Caudepón¹,
9 Santiago Pellejero¹, Santiago Miquelez¹, Anastasio Rubio¹, Elena Goñi⁴ and Araceli Hernández-Vitoria^{3, 5}
10
11

12
13
14 ¹Department of Medical Physics, Complejo Hospitalario de Navarra.

15 Calle Irunlarrea 3, 31008 Pamplona (Spain)

16
17 ²Nuclear Medicine Department, Hospital Universitario Miguel Servet

18 Paseo Isabel la Católica, 1-3 50009 Zaragoza (Spain)

19
20 ³Radiology Department, Universidad de Zaragoza

21 Calle Domingo Miral S/N 50009 Zaragoza (Spain)

22
23 ⁴Department of Nuclear Medicine, Complejo Hospitalario de Navarra.

24 Calle Irunlarrea 3, 31008 Pamplona (Spain)

25
26 ⁵Medical Physics Service, Hospital Clínico Universitario Lozano Blesa

27 Avenida San Juan Bosco, 15 50009 Zaragoza (Spain)

28
29
30
31
32
33
34 E-mail: fmaneruc@navarra.es
35
36
37
38
39
40
41
42
43
44
45
46
47
48
49
50
51
52
53
54
55
56
57
58
59
60

Abstract

Dosimetry in liver radioembolization with ^{90}Y microspheres is a fundamental tool, both for the optimization of each treatment and for improving knowledge of the treatment effects in the tissues. Different options are available for estimating the administered activity and the tumor/organ dose, among them the so-called *partition method*. The key factor in the partition method is the tumor/normal tissue activity uptake ratio (T/N), which is obtained by a Single-Photon Emission Computed Tomography (SPECT) scan during a pre-treatment simulation. The less clear the distinction between healthy and tumor parenchyma within the liver, the more difficult it becomes to estimate the T/N ratio; therefore the use of the method is limited. This study presents a methodology to calculate the T/N ratio using global information from the SPECT. The T/N ratio is estimated by establishing uptake thresholds consistent with previously performed volumetry. This dose calculation method was validated against three-dimensional voxel dosimetry, and was also compared with the standard partition method based on freehand regions of interest (ROI) outlining on SPECT slices. Both comparisons were done on a sample of 20 actual cases of hepatocellular carcinoma treated with resin microspheres. The proposed method and the voxel dosimetry give very similar results. Differences are found in several cases when comparing with results derived from the ROI method. Differences in the T/N ratio imply more difference in tumor dose than in normal liver dose. Dispersion of values is greater in the ROI-based method than in the other two. The process is very simple and avoids the subjectivity inherent to manual distinction between tumor/normal liver tissue interfaces. Dosimetry results obtained with the new method are equivalent to those provided by voxel dosimetry. Compared to the use of ROIs, it also provides greater simplicity and – most importantly – greater reproducibility.

Keywords: Radioembolization, Microspheres, Partition Method, Y90 dosimetry

Introduction

Transarterial liver radioembolization (TARE) is a form of nuclear medicine radiotherapy in which microspheres loaded with yttrium-90 are delivered to the tumor via the hepatic artery. It leverages the liver's dual blood supply to deposit a large quantity of radiation dose to the tumor without damaging the healthy parenchyma. The administered activity and the dose estimation are determined during a pre-treatment simulation involving the administration of macroaggregated albumin marked with ^{99m}Tc (^{99m}Tc -MAA), carried out according to the planned treatment, and in an immediately subsequent SPECT scan (Dezarn *et al.*, 2011).

In the case of resin spheres, the prescription methods currently available are: (I) Empirical Method, not personalized and already in disuse; (II) Body Surface Area (BSA) method, which includes patient size and liver size in an empirical equation for the calculation of activity, but does not take into account the absorbed dose; (III) Partition Method, which considers the different uptake of healthy and diseased tissue (Ho *et al.*, 1996; Sirtex *SIR-Spheres*[®] Package Insert; Kennedy *et al.*, 2012); and finally (IV) Three-Dimensional (3D) Dosimetry, which has several possibilities in development, although it is still not widespread in practice and little clinical data is available (Dezarn *et al.*, 2011; O'Doherty, 2015). The latter two are based on the MIRD schema, so they are not only prescription methods but also dose estimation methods. This dose estimation is needed to obtain a personalized prescription and treatment planning in nuclear medicine therapy and is becoming increasingly demanded (Chiesa *et al.*, 2017). Given that 3D dosimetry is not quite established in routine clinical practice, the most sophisticated method in use is usually the partition method, and it is increasingly prevalent in hospitals throughout the world. The resin microspheres manufacturer (*SIR-Spheres*[®], Sirtex Medical) suggests using the partition method in especially favorable anatomies (*Sirtex SIR-Spheres*[®] Package Insert). The Partition method is described and validated for cases where it is possible to clearly identify the border between the healthy parenchyma and the tumor (Ho *et al.*, 1996; Ho *et al.*, 1997a; Ho *et al.*, 1997b).

To perform the calculations, it is necessary to know: (I) lung shunt fraction (*LSF*), fraction of the activity injected into the patient that migrates to the lungs; (II) liver and tumor masses, obtained by volumetry in radiological imaging, (III) lung mass, usually replaced by the standard value of 1 kg; and (IV) the tumor/normal tissue ratio (*T/N*), as defined in equation (1) (Dezarn *et al.*, 2011; Sirtex *SIR-Spheres*[®] Package Insert; Giammarile *et al.*, 2011; Gulec *et al.*, 2006).

$$T / N = \frac{\left(\frac{A_{Tumor}}{m_{Tumor}} \right)}{\left(\frac{A_{NormalLiver}}{m_{NormalLiver}} \right)} \quad (1)$$

Where A_{Tumor} and $A_{NormalLiver}$ are tumor and healthy liver activity, and m_{Tumor} and $m_{NormalLiver}$ are the masses of the tumor and the healthy liver, respectively.

No single benchmark method exists to calculate the T/N ratio (Arbizu *et al.*, 2014), and recent proposals of objective observer-independent methods are conditioned by segmentation (Garin *et al.*, 2012; Lam *et al.*, 2015; Kao *et al.*, 2012; Garin *et al.*, 2013). In the standard procedure a comparison between the quotient defined in equation (1) and a normalized ratio of counts of two regions or volumes of interest on the SPECT images was performed, including tumor and healthy liver, respectively. This measure is manual and therefore presents a high degree of uncertainty, depending greatly on the criterion of the particular user performing this.

When both the partition and BSA methods are applicable, the former is considered a better choice, but presents serious limitations which impede its widespread use (Kao *et al.*, 2011). It is customary to employ the partition method only in patients selected for presenting especially clear healthy-diseased parenchyma interfaces. Only experience and knowledge of the equations of the model, its meaning and its scope, can determine the most appropriate method for each patient.

This study presents a new method, based on the partition method, by estimating the T/N ratio from the global information provided by the gamma camera imaging of ^{99m}Tc -MAA. The validity of the new method was studied in cases treated with radioembolization, comparing its results against those obtained through 3D dosimetry at the voxel level.

Methods

Estimating the tumor/normal tissue uptake ratio

In a practical way, T/N ratio it is often likened to the ratio of SPECT counts per unit surface area or volume, between tumor and normal liver (Dezarn *et al.*, 2011). For a 3D analysis, distinction between healthy and diseased tissue is needed, but this is complex on both a conceptual and technical level. For the method proposed herein, segmentation based on the SPECT count thresholds is considered valid. All voxels with counts below a lower threshold T_l are identified as nonirradiated region; voxels with counts

above an upper threshold T_2 are identified as tumor; and the rest, located between the two thresholds, is identified as treated healthy liver.

The SPECT voxel value spectrum, between a minimum (m) and a maximum (M), on an arbitrary scale, is defined by the parameters of acquisition and reconstruction. It is assumed that each voxel number of counts is proportional to the ^{90}Y activity deposited in it. This way, total counts of the study correspond to the total administered activity. Similarly, the sum of counts of all the voxels with $T_1 \leq i < T_2$ corresponds to the activity in the normal liver, and the sum of counts of all the voxels with $i \geq T_2$ corresponds to the activity in the tumor. The grey level histogram of the 3D matrix shows the frequency of voxels, f_i , that are assigned each value of spectrum i , from $i=m$ to $i=M$ (figure 1). Thus, the sum of counts of a range (a, b) is:

$$\text{Counts}(a,b) = \sum_{i=a}^b i \cdot f_i \quad (2)$$

Given that the sum of counts in each voxel is proportional to the activity contained in it, where k is the proportionality constant, the activity in the volumes of interest can be determined:

$$A_{\text{Total}} = k \cdot \sum_{i=m}^M i \cdot f_i \quad (3)$$

$$A_{\text{NormalLiver}} = k \cdot \sum_{i=T_1}^{T_2-1} i \cdot f_i \quad (4)$$

$$A_{\text{Tumor}} = k \cdot \sum_{i=T_2}^M i \cdot f_i \quad (5)$$

Knowing the voxel volume, V_{voxel} , and the number of voxels between the thresholds, healthy liver and tumor volume can be expressed as:

$$V_{\text{NormalLiver}} = V_{\text{voxel}} \cdot \sum_{i=T_1}^{T_2-1} f_i \quad (6)$$

$$V_{\text{Tumor}} = V_{\text{voxel}} \cdot \sum_{i=T_2}^M f_i \quad (7)$$

Optimal thresholds for each patient were chosen so as to verify equations (6) and (7). That is, threshold values were selected so that the volume of all the voxels with counts over T_1 and T_2 include the volume obtained in the previous liver and tumor volumetry, respectively.

On first approximation, the mass densities of the tumor and the healthy parenchyma can be considered equal. This allows for the identification of the ratio of masses from the T/N definition in the ratio of the volumes defined in equations (6) and (7). When applying the theoretical definition of the T/N ratio (equation (1)), the 3D T/N uptake ratio, T/N_{3D} , can be defined as:

$$T / N_{3D} = \frac{\left(\frac{\sum_{i=T_2}^M i \cdot f_i}{V_{\text{voxel}} \cdot \sum_{i=T_2}^M f_i} \right)}{\left(\frac{\sum_{i=T_1}^{T_2-1} i \cdot f_i}{V_{\text{voxel}} \cdot \sum_{i=T_1}^{T_2-1} f_i} \right)} \quad (8)$$

The T/N_{3D} estimation method should be valid in all cases for which the following conditions are verified:

(I) clear uptake of activity throughout the entire liver or in one of lobes; (II) the most marked uptake foci located in the areas with tumor presence in diagnostic imaging; and (III) absence of significant extrahepatic leaks.

The T/N_{3D} ratio thus calculated does not differ conceptually in any respect to the T/N ratio commonly used in the partition method. It is simply a more realistic way of calculating the parameter, which is then included in the model's dose calculation without modification.

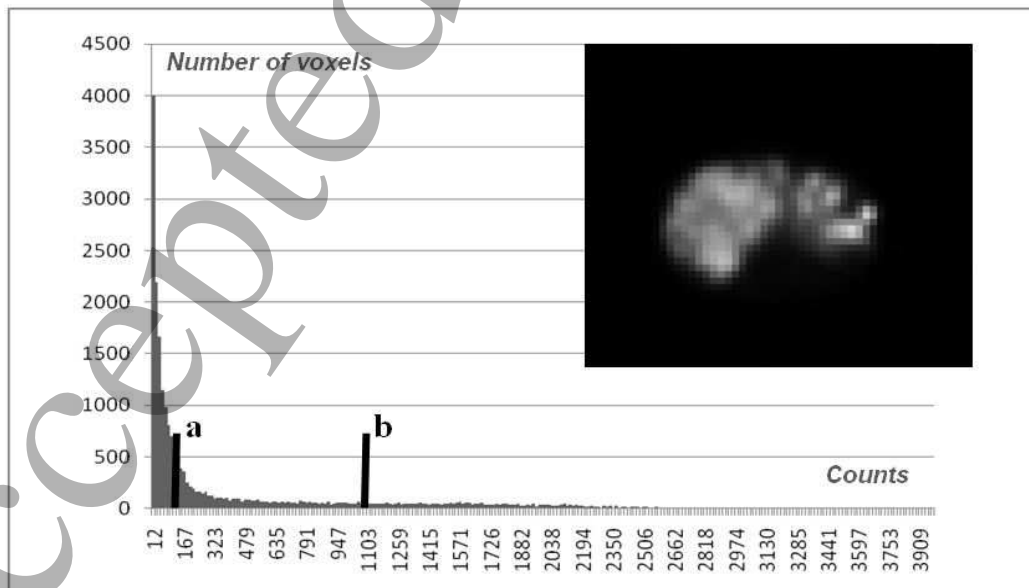


Figure 1 Grey level histogram of ^{99m}Tc -MAA SPECT image (axial slice shown in upper right inset). Vertical lines mark the range of values (a, b) in which the sum of counts should be obtained.

Selected cases

The proposed calculation method was implemented retrospectively in a group of 20 cases of hepatocellular carcinoma treated with resin spheres at our centre between August 2011 and October 2015.

For comparative purposes, the T/N ratio was estimated for this group with two other methods (ROI drawing on axial slices of SPECT and with voxel dosimetry). Only cases for which the tumor was sufficiently identifiable as to calculate the T/N ratio using ROIs in a reliable manner were selected. Table 1 shows the characteristics of the 20 cases that met the criteria.

Case	$V_{Total\ Liver} (cm^3)$	$V_{Tumor} (cm^3)$	LSF
1	1490	25	11%
2	1399	189	4%
3	863	52	8%
4	863	52	5%
5	1056	20	2%
6	2538	8	6%
7	2050	28	3%
8	1248	4	3%
9	1327	10	6%
10	1845	355	3%
11	1356	15	7%
12	772	115	7%
13	1027	15	8%
14	1683	17	8%
15	1006	10	6%
16	1385	30	2%
17	1907	38	7%
18	1407	47	6%
19	1427	77	7%
20	1107	172	10%

Table 1 Anatomical data of selected cases for T/N and dose calculation.

SPECT-CT acquisition was conducted using an Infinia Hawkeye 4 (General Electric Healthcare) model dual-head gamma camera. LEHR (Low Energy High Resolution) collimators were used, and ^{99m}Tc energy peak was selected. 64 projections (64 x 64, 25 s per projection) were acquired. Attenuation correction was applied. Images were reconstructed with the OSEM (ordered subset expectation maximization) algorithm. Liver and tumor volumetry were carried out using the diagnostic CT scans. Lung shunt fraction was calculated based on planar gamma camera imaging according to the standard procedure (Dezarn *et al.*, 2011; Giammarile *et al.*, 2011).

Comparison between methods

In the new method proposed in this study, the T/N_{3D} ratio was calculated using the 3D voxel matrix of SPECT, according to the definition of equation (8). Each voxel belongs to one and only one of the three distinct subsets: tumor voxels, healthy liver voxels and all other voxels. The thresholds which verified the conditions established by equations (6) and (7) were chosen to delimit the subsets, T_1 and T_2 , respectively. Optimal thresholds were obtained for each patient by an iterative computation process as explained below:

An initial test threshold t_0 was established as the maximum value of the spectrum (M). Next, a test liver volume V_0 was computed by summing up the volume of all the voxels with counts $i > t_0$ and a comparison with the known volume $V_{TotalLiver}$ was made. Successive test thresholds t_j were then selected and associated test volumes V_j were calculated for the next iterations:

$$t_j = t_{j-1} + (M/2^j) \quad \text{if } V_{j-1} < V_{TotalLiver} \quad (9)$$

$$t_j = t_{j-1} - (M/2^j) \quad \text{if } V_{j-1} > V_{TotalLiver} \quad (10)$$

After “ n ” iterations (being n the number of the image bits), the definitive liver volume $V_n = V_{TotalLiver}$ was obtained, from which the optimal threshold $T_1 = t_n$ was established. The same process was repeated for achieving a T_2 threshold to fit a known tumor volume (V_{Tumor}). Both the T/N_{3D} value and its corresponding threshold were computed with in-house software specifically developed to this end with the Python programming language (Python Software Foundation).

The second way of estimating the T/N ratio was the traditional method using ROIs (T/N_{ROI}). The counts in 5 ROIs representative of healthy tissue and another 5 with tumor foci were measured on axial slices of the SPECT.

The third way to estimate the T/N ratio was the voxel S-value approach (VSV), carried out using a convolution of the ^{99m}Tc -MAA activity matrix with a kernel for ^{90}Y , in accordance with the following equation (Dezarn *et al.*, 2011; Bolch *et al.*, 1999):

$$\mathbf{D} = \tilde{\mathbf{A}} \otimes \mathbf{K} \quad (11)$$

Where \mathbf{D} is the absorbed dose matrix, $\tilde{\mathbf{A}}$ is the matrix of accumulated activity obtained from the ^{99m}Tc -MAA, and \mathbf{K} is the spatial distribution of S factors at the voxel level, which acts as the convolution kernel. The count transformation in activity is performed by normalizing the value of each voxel (C_i) with respect to the total counts in the treated liver, according to the equation (12) (Sarfaraz *et al.*, 2004):

$$A_i = A_{Total} \frac{C_i}{(C_{Total} - C_{Background})} \quad (12)$$

Where A_i is the administered activity in each voxel, A_{Total} is the total activity in the liver (administered activity minus lung shunt), C_{Total} is the sum of counts of all SPECT voxels, and $C_{Background}$ is the sum of counts of all voxels outside the treated volume (i. e., outside the liver and tumor, including all the voxels outside the patient). The employed kernel was downloaded from the *S values for voxel dosimetry* online database (Lanconelli *et al.*, 2012). It was used corresponding to ^{90}Y with a spacing of 2.21 mm. Manipulation of DICOM files, transformation of counts in accumulated activity and convolution were carried out with in-house software developed with the Python programming language (Mañeru *et al.*, 2015). Once the spatial dose distribution was known, the tumor was identified by locating the area with the highest dose until the known tumor size was reached. Of the remaining volume, the normal liver was identified, in turn, by locating the area with the highest dose until the healthy parenchyma size was reached. The calculation of the T/N (T/N_{VSV}) ratio is reduced to the quotient between the mean dose in the tumor and in the healthy liver.

Voxel dosimetry was considered the most reliable of the three methods of dose estimation, and so T/N_{VSV} was used as the reference in the comparison.

Results

The T/N_{3D} ratio was estimated according to the new method for the selected cases. Likewise, the T/N ratio was estimated using ROIs on the SPECT (T/N_{ROI}) and voxel dosimetry (T/N_{VSV}). Table 2 shows the thresholds and the T/N ratio values obtained. Relatively little spread can be seen in the T/N ratio values; the range of all the values of the three methods is between 1.7 and 7.5. VSV method has a range between

1
2
3 1.7 and 5.7, with an average value of 3.5. Eighty percent of the values are between 2 and 5, in accordance
4 with both theoretical expectations and expectations based on comparison with other publications (Gulec
5 *et al.*, 2009; Campbell *et al.*, 2009). The value obtained by the ROI method moves significantly away
6 from the other two in a number of cases, although on average there is not much difference (3% difference
7 between the 3D method and the VSV method, and 7% difference between the ROI method and the VSV
8 method, in both cases providing a higher value). Figure 2 illustrates all this in a graph.
9
10
11
12
13

Case	Threshold		T/N		
	T_1	T_2	3D	ROI	VSV
1	1310	32700	5.71	7.50	5.68
2	1900	10700	2.84	2.45	2.72
3	5000	24000	2.54	2.02	2.46
4	4300	28500	2.71	2.93	2.64
5	1760	32760	4.14	5.69	4.11
6	680	10300	5.53	3.10	5.12
7	1265	7950	3.36	2.32	3.26
8	2025	16350	3.33	3.27	3.30
9	1765	9800	2.49	2.31	2.42
10	1218	5180	2.66	3.09	2.62
11	900	7900	4.88	3.58	4.65
12	1555	3515	1.91	2.08	1.88
13	2240	17500	3.71	3.18	3.50
14	1173	16100	4.76	4.85	4.66
15	2620	28000	4.63	4.79	4.49
16	1010	14850	3.67	4.62	3.47
17	815	11320	4.79	6.35	4.66
18	1510	10200	3.67	5.93	3.52
19	1150	9920	3.90	3.59	3.80
20	2865	6820	1.73	2.07	1.72

14
15
16
17
18
19
20
21
22
23
24
25
26
27
28
29
30
31
32
33
34
35
36
37
38
39
40
41
42
43
44
45
46
47
48 **Table 2** Thresholds values used for the calculation of T/N_{3D} and values of the T/N ratio obtained through
49 the three methods.
50
51
52
53

54 Knowing lung shunt, liver and tumor volumes and the T/N ratio, the partition method equations are used
55 to immediately deduce the mean doses to the tumor and the healthy liver. Figures 3 and 4 contain the
56
57
58
59
60

1
2
3
4
5
6
7
8
9
10
11
12
13
14
15
16
17
18
19
20
21
22
23
24
25
26
27
28
29
30
31
32
33
34
35
36
37
38
39
40
41
42
43
44
45
46
47
48
49
50
51
52
53
54
55
56
57
58
59
60

dosimetry results with the new method and the two used for comparison, expressed in units of dose /activity (Gy/GBq).

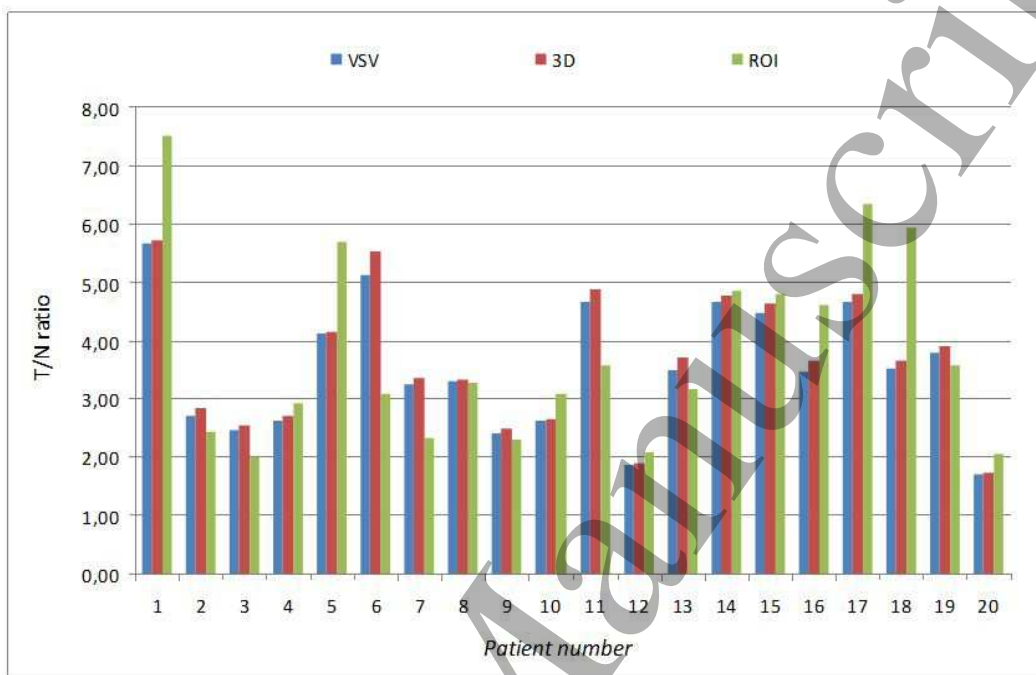


Figure 2 Values of the T/N ratio obtained in the three compared methods

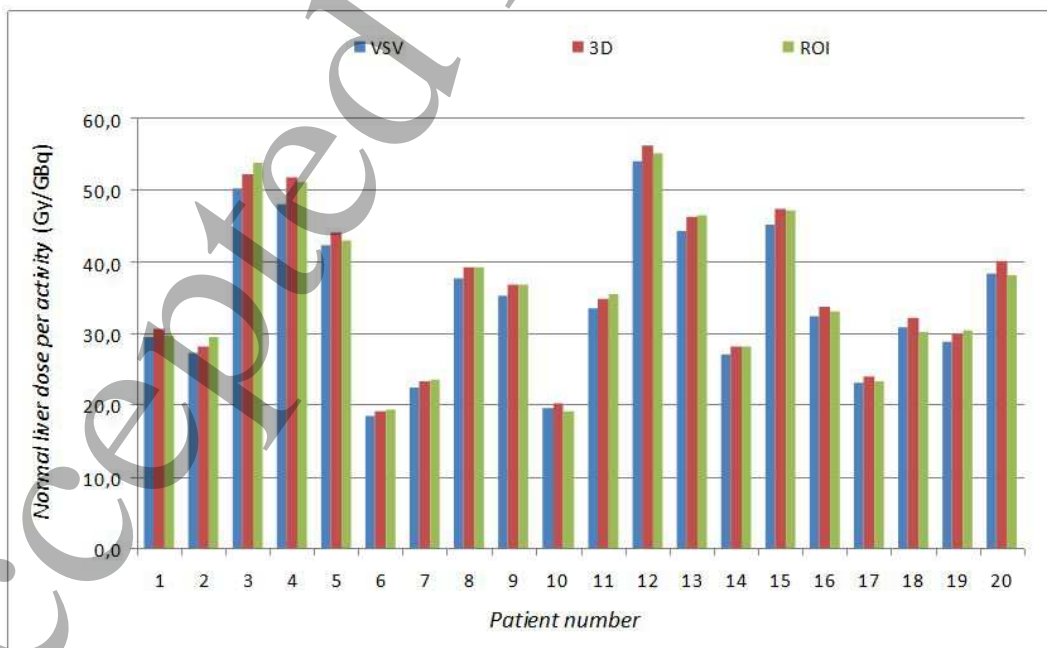


Figure 3 Dose per unit of ⁹⁰Y activity administered in healthy liver.

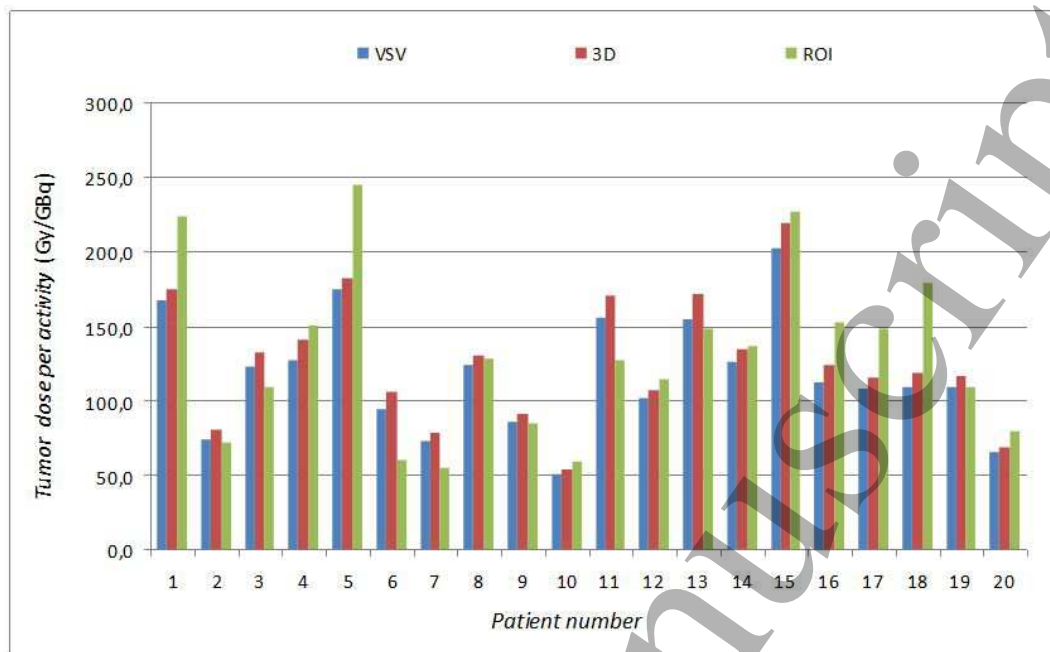


Figure 4 Dose per unit of ^{90}Y activity administered in tumor.

Discussion

The partition method assumes the validity of the simulation with $^{99\text{m}}\text{Tc}$ -MAA, although the identification of the behavior of the macroaggregates with that of the microspheres remains a controversial topic today (Ulrich *et al.*, 2013; Wondergem *et al.*, 2013; Lam *et al.*, 2015; Chiesa *et al.*, 2014). However, according to the current state of the art, there is no other alternative but to accept this equivalence, and it is considered generally valid (Garin, 2015; Braat *et al.*, 2015; Garin *et al.*, 2015).

The only current possibility for calculating the T/N ratio before treatment is by extracting the information from the $^{99\text{m}}\text{Tc}$ -MAA SPECT. The limitations of this simulation completely condition any calculation derived from it. The activity distribution in the liver is not uniform, consistent with the local differences of microsphere concentration. Different areas are supplied by different blood vessels, each with its own blood flow (Uliel *et al.*, 2012). Each lesion has a specific uptake, sometimes in different ways within the same patient. Even within large lesions, areas of different uptake appear due to the different vascularization or the lack thereof in the case of necrosis. This distribution, full of gradients and local maxima and minima, is not easy to simplify by dividing the total liver volume into 2 separate areas (healthy and sick). It is even more difficult to do so with a small number of ROIs, which should be identified with representative parts from both areas, excluding from the analysis the rest of the activity

1
2
3 map. Using these ROIs leaves aside most of the information contained in the SPECT, which is already
4 limited in itself. Only a calculation of the T/N ratio using the complete SPECT, as proposed in this study,
5 will include all the details provided by the ^{99m}Tc -MAA SPECT in the resulting value. In this way, the T/N
6 ratio and the partition method can be brought to a higher level of accuracy. The mean dose values
7 obtained will be as true to reality as the applied division between the healthy and diseased areas. For this
8 work, this division was based on a previous volumetry derived from diagnostic CT images. However,
9 other alternatives can also be considered. We believe that direct VOI drawing on SPECT-CT images
10 presents several practical problems. A CT gamma camera cannot always provide images with the same
11 quality as those obtained when diagnostic equipment is used. Registration between both CT images is
12 possible, although a perfect anatomical coincidence is difficult: internal movements and changes in the
13 position of the patient can result in significant differences. Nevertheless, the size of the liver and of the
14 tumor will be the same despite liver deformations, and thus a reliable volumetry can be always taken as
15 valid. The threshold selection from grey-level histograms is another possible alternative. The latter is a
16 very useful segmentation technique in nuclear medicine imaging; unfortunately, the ^{99m}Tc -MAA SPECT
17 images analysed in this work did not show any pattern as to allow the determination of a threshold value
18 in the histogram. All these considerations led us to accept the volumetry data as a robust start point for
19 segmentation.

20
21
22
23
24
25
26
27
28
29
30
31
32
33
34 The new partition method (based on T/N_{3D}) and the reference (T/N_{VSV}) give very similar results. The
35 differences found, both in the T/N ratio and in the absorbed dose, are minimal compared to other
36 uncertainties of the process. We therefore present the T/N_{3D} ratio calculation as a very reliable method for
37 estimating the mean dose. A detailed analysis of the results shows that the T/N_{3D} ratio is slightly higher
38 than T/N_{VSV} in all cases. To some extent, this could be due to the difference caused by using the local
39 energy deposition approach respect instead of a convolution method (Pasciak *et al.*, 2014). The use of the
40 partition method (T/N_{3D}) implies acceptance of local deposition, and consequently does not consider the
41 difference between a defined tumor focus and several dispersed foci. In the first case, the high uptake
42 voxels would be near each other, and the dose scattered from these areas would contribute mainly to the
43 rest of the next high activity voxels. In contrast, in the case of dispersed foci, a greater number of high
44 activity voxels would contribute to the dose in the voxels considered to be healthy tissue. The size of the
45 tumor, the tumor grouping or dispersal and the voxel size are factors that would determine the amount of
46 this effect, which is not easy to model. The partial volume effect will therefore be different for different
47
48
49
50
51
52
53
54
55
56
57
58
59
60

1
2
3 distributions of activity. On the other hand, the way to estimate the background in the voxel dosimetry
4 calculation (equation (12)) introduces a normalization in the calculation of the dose distribution that can
5 also have an influence on this systematic difference between the value pairs of the T/N ratio.
6
7

8 It also shows that, on average, $T/N_{3D} < T/N_{ROI}$, being the most marked difference in cases in which the
9 standard method offers higher values for the T/N ratio. The cause of this behavior should be associated
10 with the characteristics of the tumor distribution, but a cause-effect relationship between the initial data
11 (administered activity and tumor and organ volumes) and this difference has not been found. Given that it is
12 more pronounced in cases with a higher value for T/N_{ROI} , it seems reasonable to ascribe this deviation to
13 the limitations of the ROI-based method in more extreme cases. Because of this, a more accurate tumor
14 dose estimation should be expected when using this method.
15
16
17
18
19
20

21 We have seen that the major differences in the T/N ratio do not necessarily imply appreciable differences
22 in the dose to the healthy liver, while the values of the dose to the tumor are more influenced by the
23 variation of the T/N ratio. This suggests that any errors in the estimation of the T/N ratio can have
24 significant influence in the calculation of doses to the tumor but little influence in the calculation of doses
25 to healthy tissue. The risk of toxicity in normal hepatic tissue is the main parameter determining the
26 administered activity in patients who undergo radioembolization. With this in mind, it may seem that the
27 proposed method does not improve the accuracy of normal liver dose; however, the comparison with the
28 standard T/N estimation was performed only in special cases (those for which the drawing of the ROI is
29 feasible). The potential candidate cases for using the described methodology are all those that comply
30 with conditions (I), (II), and (III), that is, more than the ones that are normally considered suitable for the
31 use of the partition method. A better understanding on the absorbed dose in tumor and healthy liver will
32 enable more personalized treatments. A growing number of patients for whom the alternative is the BSA
33 method could benefit with such a personalized treatment planning via the partition method.
34
35
36
37
38
39
40
41
42
43
44

45 The dispersion of values of any of the three dosimetric parameters, represented by the standard deviation
46 is greater in the ROI-based method than in the other two. It is thus clear that the dose data calculated from
47 T/N_{ROI} , in addition to deviating more from the reference value, are less reproducible than those calculated
48 from T/N_{3D} . This is particularly striking when applying the ROI method in such a controlled manner as
49 was done in this study, where a uniform criterion was followed to contour ROIs. Different people, in
50 different centers, with different tools, will increase the real dispersion in the estimate of T/N_{ROI} . In this
51 context, the presented method for estimating the tumor-to-liver uptake ratio as T/N_{3D} is extremely
52
53
54
55
56
57
58
59
60

1
2
3 reproducible, because it only has the liver and tumor volumes as variables. It is true that they are not
4 always easy to measure, but that challenge is also present in the standard ROI method (Ilhan *et al.*, 2015).
5
6 More reproducibility is a great advantage since it shortens the learning curve, prevents human error and
7
8 allows for a more reliable exchange of data between centers.
9

10
11 Implicitly, using the new method based on T/N_{3D} implies accepting tumor and liver segmentation based
12 on uptake thresholds in the ^{99m}Tc -MAA SPECT. The delimitation of volumes from thresholds has a very
13
14 solid conceptual foundation in the field of radioembolization; the requirement that the areas of higher
15
16 uptake coincide with the areas of the highest tumor activity is precisely one of the reasons this therapy is
17
18 effective (Kao *et al.*, 2012; Uliel *et al.*, 2012). The other major requirement, the absence of extrahepatic
19
20 leaks, is a cause of contraindication for the treatment, for which reason it is also a fully justified condition
21
22 (Lau *et al.*, 2012; Kennedy *et al.*, 2007). In the case of existing low uptake necrotic zones, the method
23
24 proposed here is an advantage since the calculation does not ever include them in the tumor (and not even
25
26 in the healthy liver if signal is small enough).

27
28 The described method is based on the ^{99m}Tc -MAA as a surrogate of the behavior of the microspheres, but
29
30 this does not preclude it from being similarly applicable to the post-treatment dosimetry based on PET
31
32 (Braat *et al.*, 2015; Srinivas *et al.*, 2014; Pasciak *et al.*, 2014).
33

34 **Conclusion**

35
36 We present a new method for calculating the activity uptake ratio between the tumor and the healthy
37
38 tissue, taking into account the full influence of the SPECT scan prior to treatment. The results obtained
39
40 with this method, in terms of mean dose in tumor and liver, are comparable to those achieved with the
41
42 VSV method which can be considered as a reference. If the prescription of treatment is performed using
43
44 the mean dose in the tumor, as is usually done in practice, the simplicity and reproducibility of the
45
46 proposed method makes it an excellent option for calculating the administered activity.
47

48 **REFERENCES**

- 49
50
51 Arbizu J, Rodriguez-Fraile M, Martí-Climent J, Dominguez-Prado I and Vigil C 2014 *Liver Nuclear*
52 *Medicine Procedures for Treatment Evaluation and Administration. Radioembolization with ^{90}Y*
53 *Microspheres*, ed J Bilbao and M Reiser: Springer
54
55 Bolch W E, Bouchet L G, Robertson J S, Wessels B W, Siegel J A, Howell R W, Erdi A K, Aydogan B,
56 Costes S, Watson E E, Brill A B, Charkes N D, Fisher D R, Hays M T and Thomas S R 1999
57 MIRDO pamphlet No. 17: the dosimetry of nonuniform activity distributions--radionuclide S
58 values at the voxel level. Medical Internal Radiation Dose Committee *J Nucl Med* **40** 11S-36S
59
60

- 1
2
3 Braat A J, Smits M L, Braat M N, van den Hoven A F, Prince J F, de Jong H W, van den Bosch M A and
4 Lam M G 2015 90Y Hepatic Radioembolization: An Update on Current Practice and Recent
5 Developments *J Nucl Med* **56** 1079-87
- 6 Campbell J M, Wong C O, Muzik O, Marples B, Joiner M and Burmeister J 2009 Early dose response to
7 yttrium-90 microsphere treatment of metastatic liver cancer by a patient-specific method using
8 single photon emission computed tomography and positron emission tomography *Int J Radiat
9 Oncol Biol Phys* **74** 313-20
- 10 Chiesa C, Lambert B, Maccauro M, Ezziddin S, Ahmadzadehfar H, Dieudonné A, Cremonesi M,
11 Konijnenberg M, Lassmann M, Pettinato C, Strigari L, Vanderlinden B, Crippa F, Flamen P and
12 Garin E 2014 Pretreatment Dosimetry in HCC Radioembolization with (90)Y Glass
13 Microspheres Cannot Be Invalidated with a Bare Visual Evaluation of (99m)Tc-MAA Uptake of
14 Colorectal Metastases Treated with Resin Microspheres *J Nucl Med* **55** 1215-6
- 15 Chiesa C, Sjögreen Gleisner K, Flux G, Gear J, Walrand S, Bacher K, Eberlein U, Visser E P, Chouin N,
16 Ljungberg M, Bardiès M, Lassmann M, Strigari L and Konijnenberg M W 2017 The conflict
17 between treatment optimization and registration of radiopharmaceuticals with fixed activity
18 posology in oncological nuclear medicine therapy *Eur J Nucl Med Mol Imaging*
- 19 Dezar W A, Cessna J T, DeWerd L A, Feng W, Gates V L, Halama J, Kennedy A S, Nag S, Sarfaraz M,
20 Sehgal V, Selwyn R, Stabin M G, Thomadsen B R, Williams L E and Salem R 2011
21 Recommendations of the American Association of Physicists in Medicine on dosimetry,
22 imaging, and quality assurance procedures for 90Y microsphere brachytherapy in the treatment
23 of hepatic malignancies *Med Phys* **38** 4824-45
- 24 Garin E 2015 Radioembolization with (90)Y-loaded microspheres: high clinical impact of treatment
25 simulation with MAA-based dosimetry *Eur J Nucl Med Mol Imaging* **42** 1189-91
- 26 Garin E, Lenoir L, Edeline J, Laffont S, Mesbah H, Porée P, Sulpice L, Boudjema K, Mesbah M,
27 Guillygomarc'h A, Quehen E, Pracht M, Raoul J L, Clément B, Rolland Y and Boucher E 2013
28 Boosted selective internal radiation therapy with 90Y-loaded glass microspheres (B-SIRT) for
29 hepatocellular carcinoma patients: a new personalized promising concept *Eur J Nucl Med Mol
30 Imaging* **40** 1057-68
- 31 Garin E, Lenoir L, Rolland Y, Edeline J, Mesbah H, Laffont S, Porée P, Clément B, Raoul J L and
32 Boucher E 2012 Dosimetry based on 99mTc-macroaggregated albumin SPECT/CT accurately
33 predicts tumor response and survival in hepatocellular carcinoma patients treated with 90Y-
34 loaded glass microspheres: preliminary results *J Nucl Med* **53** 255-63
- 35 Garin E, Rolland Y, Laffont S and Edeline J 2015 Clinical impact of (99m)Tc-MAA SPECT/CT-based
36 dosimetry in the radioembolization of liver malignancies with (90)Y-loaded microspheres *Eur J
37 Nucl Med Mol Imaging*
- 38 Giammarile F, Bodei L, Chiesa C, Flux G, Forrer F, Kraeber-Bodere F, Brans B, Lambert B,
39 Konijnenberg M, Borson-Chazot F, Tennvall J, Luster M and Therapy O c a D C 2011 EANM
40 procedure guideline for the treatment of liver cancer and liver metastases with intra-arterial
41 radioactive compounds *Eur J Nucl Med Mol Imaging* **38** 1393-406
- 42 Gulec S A, Mesoloras G and Stabin M 2006 Dosimetric techniques in 90Y-microsphere therapy of liver
43 cancer: The MIRD equations for dose calculations *J Nucl Med* **47** 1209-11
- 44 Gulec S A, Selwyn R, Weiner R, Flamen P, Mesoloras G, Lamonica D, Machac J, Hiatt G, Ugur O and
45 McGoron A 2009 Radiomicrosphere Therapy: Nuclear Medicine Considerations, Guidelines,
46 and Protocols. *Journal of Interventional Oncology* **2** 16
- 47 Ho S, Lau W Y, Leung T W, Chan M, Chan K W, Lee W Y, Johnson P J and Li A K 1997a Tumour-to-
48 normal uptake ratio of 90Y microspheres in hepatic cancer assessed with 99Tcm
49 macroaggregated albumin *Br J Radiol* **70** 823-8
- 50 Ho S, Lau W Y, Leung T W, Chan M, Johnson P J and Li A K 1997b Clinical evaluation of the partition
51 model for estimating radiation doses from yttrium-90 microspheres in the treatment of hepatic
52 cancer *Eur J Nucl Med* **24** 293-8
- 53 Ho S, Lau W Y, Leung T W, Chan M, Ngar Y K, Johnson P J and Li A K 1996 Partition model for
54 estimating radiation doses from yttrium-90 microspheres in treating hepatic tumours *Eur J Nucl
55 Med* **23** 947-52
- 56 Ilhan H, Görötschan A, Paprottka P, Jakobs T F, Fendler W P, Bartenstein P, Hacker M and Haug A R
57 2015 Systematic evaluation of tumoral 99mTc-MAA uptake using SPECT and SPECT/CT in
58 502 patients before 90Y radioembolization *J Nucl Med* **56** 333-8
- 59 Kao Y H, Hock Tan A E, Burgmans M C, Irani F G, Khoo L S, Gong Lo R H, Tay K H, Tan B S, Hoe
60 Chow P K, Eng Ng D C and Whatt Goh A S 2012 Image-guided personalized predictive
dosimetry by artery-specific SPECT/CT partition modeling for safe and effective 90Y
radioembolization *J Nucl Med* **53** 559-66

- 1
2
3 Kao Y H, Tan E H, Ng C E and Goh S W 2011 Clinical implications of the body surface area method
4 versus partition model dosimetry for yttrium-90 radioembolization using resin microspheres: a
5 technical review *Ann Nucl Med* **25** 455-61
- 6 Kennedy A, Coldwell D, Sangro B, Wasan H and Salem R 2012 Radioembolization for the treatment of
7 liver tumors general principles *Am J Clin Oncol* **35** 91-9
- 8 Kennedy A, Nag S, Salem R, Murthy R, McEwan A J, Nutting C, Benson A, Espat J, Bilbao J I, Sharma
9 R A, Thomas J P and Coldwell D 2007 Recommendations for radioembolization of hepatic
10 malignancies using yttrium-90 microsphere brachytherapy: a consensus panel report from the
11 radioembolization brachytherapy oncology consortium *Int J Radiat Oncol Biol Phys* **68** 13-23
- 12 Lam M G, Banerjee A, Goris M L, Iagaru A H, Mittra E S, Louie J D and Sze D Y 2015 Fusion dual-
13 tracer SPECT-based hepatic dosimetry predicts outcome after radioembolization for a wide
14 range of tumour cell types *Eur J Nucl Med Mol Imaging* **42** 1192-201
- 15 Lanconelli N, Pacilio M, Lo Meo S, Botta F, Di Dia A, Aroche A T, Pérez M A and Cremonesi M 2012
16 A free database of radionuclide voxel S values for the dosimetry of nonuniform activity
17 distributions *Phys Med Biol* **57** 517-33
- 18 Lau W Y, Kennedy A S, Kim Y H, Lai H K, Lee R C, Leung T W, Liu C S, Salem R, Sangro B, Shuter B
19 and Wang S C 2012 Patient selection and activity planning guide for selective internal
20 radiotherapy with yttrium-90 resin microspheres *Int J Radiat Oncol Biol Phys* **82** 401-7
- 21 Mañeru F, Otal A, Gracia M, Gallardo N, Olasolo J, Fuentemilla N, Bragado L, Martin-Albina M,
22 Lozares S, Pellejero S, Miquelez S and Rubio A 2015 SU-E-T-02: 90Y Microspheres Dosimetry
23 Calculation with Voxel-S-Value Method: A Simple Use in the Clinic *Med Phys* **42** 3330
- 24 O'Doherty J 2015 A review of 3D image-based dosimetry, technical considerations and emerging
25 perspectives in 90Y microsphere therapy. *Journal of Diagnostic Imaging in Therapy*
- 26 Pasciak A S, Bourgeois A C and Bradley Y C 2014 A Comparison of Techniques for (90)Y PET/CT
27 Image-Based Dosimetry Following Radioembolization with Resin Microspheres *Front Oncol* **4**
28 121
- 29 Sarfaraz M, Kennedy A S, Lodge M A, Li X A, Wu X and Yu C X 2004 Radiation absorbed dose
30 distribution in a patient treated with yttrium-90 microspheres for hepatocellular carcinoma *Med*
31 *Phys* **31** 2449-53
- 32 Sirtex *SIR-Spheres*® Package Insert <http://www.sirtex.com>.
- 33 Srinivas S M, Natarajan N, Kuroiwa J, Gallagher S, Nasr E, Shah S N, DiFilippo F P, Obuchowski N,
34 Bazerbashi B, Yu N and McLennan G 2014 Determination of Radiation Absorbed Dose to
35 Primary Liver Tumors and Normal Liver Tissue Using Post-Radioembolization (90)Y PET
36 *Front Oncol* **4** 255
- 37 Uliel L, Royal H D, Darcy M D, Zuckerman D A, Sharma A and Saad N E 2012 From the angio suite to
38 the γ -camera: vascular mapping and 99mTc-MAA hepatic perfusion imaging before liver
39 radioembolization--a comprehensive pictorial review *J Nucl Med* **53** 1736-47
- 40 Ulrich G, Dudeck O, Furth C, Ruf J, Grosser O S, Adolf D, Stiebler M, Ricke J and Amthauer H 2013
41 Predictive value of intratumoral 99mTc-macroaggregated albumin uptake in patients with
42 colorectal liver metastases scheduled for radioembolization with 90Y-microspheres *J Nucl Med*
43 **54** 516-22
- 44 Wondergem M, Smits M L, Elschot M, de Jong H W, Verkooijen H M, van den Bosch M A, Nijssen J F
45 and Lam M G 2013 99mTc-macroaggregated albumin poorly predicts the intrahepatic
46 distribution of 90Y resin microspheres in hepatic radioembolization *J Nucl Med* **54** 1294-301
- 47
48
49
50
51
52
53
54
55
56
57
58
59
60

ACCEPTED MANUSCRIPT

Dosimetry and prescription in liver radioembolization with ^{90}Y microspheres: 3D calculation of tumor-to-liver ratio from global $^{99\text{m}}\text{Tc}$ -MAA SPECT information

To cite this article before publication: Fernando Mañeru *et al* 2017 *Phys. Med. Biol.* in press <https://doi.org/10.1088/1361-6560/aa9536>

Manuscript version: Accepted Manuscript

Accepted Manuscript is “the version of the article accepted for publication including all changes made as a result of the peer review process, and which may also include the addition to the article by IOP Publishing of a header, an article ID, a cover sheet and/or an ‘Accepted Manuscript’ watermark, but excluding any other editing, typesetting or other changes made by IOP Publishing and/or its licensors”

This Accepted Manuscript is © 2017 Institute of Physics and Engineering in Medicine.

During the embargo period (the 12 month period from the publication of the Version of Record of this article), the Accepted Manuscript is fully protected by copyright and cannot be reused or reposted elsewhere.

As the Version of Record of this article is going to be / has been published on a subscription basis, this Accepted Manuscript is available for reuse under a CC BY-NC-ND 3.0 licence after the 12 month embargo period.

After the embargo period, everyone is permitted to use copy and redistribute this article for non-commercial purposes only, provided that they adhere to all the terms of the licence <https://creativecommons.org/licenses/by-nc-nd/3.0>

Although reasonable endeavours have been taken to obtain all necessary permissions from third parties to include their copyrighted content within this article, their full citation and copyright line may not be present in this Accepted Manuscript version. Before using any content from this article, please refer to the Version of Record on IOPscience once published for full citation and copyright details, as permissions will likely be required. All third party content is fully copyright protected, unless specifically stated otherwise in the figure caption in the Version of Record.

View the [article online](#) for updates and enhancements.